

Duty ratio modulation direct torque control of brushless doubly-fed machines

Li Bing, Liu Shi, Long Teng & Zhang Jia

To cite this article: Li Bing, Liu Shi, Long Teng & Zhang Jia (2017) Duty ratio modulation direct torque control of brushless doubly-fed machines, *Automatika*, 58:4, 479-486, DOI: [10.1080/00051144.2017.1343421](https://doi.org/10.1080/00051144.2017.1343421)

To link to this article: <https://doi.org/10.1080/00051144.2017.1343421>



© 2018 The Author(s). Published by Informa UK Limited, trading as Taylor & Francis Group.



Published online: 05 Jun 2018.



Submit your article to this journal [↗](#)



Article views: 283



View related articles [↗](#)



View Crossmark data [↗](#)



Duty ratio modulation direct torque control of brushless doubly-fed machines

Li Bing^a, Liu Shi^b, Long Teng^c and Zhang Jia^d

^aSchool of Energy, Power And Mechanical Engineering, North China Electric Power University, Beijing, People's Republic of China; ^bControl and Computer Engineering College, North China Electric Power University, Beijing, People's Republic of China; ^cDepartment of Engineering, University of Cambridge, Cambridge, UK; ^dElectrical Engineering & Energy College, Tianjin Sino-German University of Applied Science, Tianjin, People's Republic of China

ABSTRACT

For the brushless doubly-fed machine (BDFM), traditional direct torque control (DTC) has many problems such as big output torque ripple and uncertain inverter switch frequency. Based on the analysis of traditional DTC, this paper proposed a new torque control which applied duty ratio modulation into direct torque control. This new control method can decrease the torque ripple effectively by adding zero voltage in each control cycle. According to the brushless BDFM state equation and the prediction of torque, flux linkage in the next moment and the theory of electromagnetic torque equals to referenced value at the instant moment in one control cycle, torque ripple can be decreased. Through theoretical analysis and experiments, the proposed control method has all advantages of traditional direct torque control and can decrease torque ripple and flux linkage ripple, which can optimize the performance of direct torque control.

ARTICLE HISTORY

Received 13 August 2016
Accepted 3 June 2017

KEYWORDS

BDFM; duty ratio modulation; torque ripple; model predictive control; direct torque control

1. Introduction

Brushless doubly fed machine (BDFM) is a new type of machine and is widely concerned in recent years. This machine is composed of two sets of independent stator winding with different pole pairs (power winding and control winding) and special rotator. Power winding is powered by power grid directly and the frequency converter powers the control winding. The advantages of BDFM are simple structure, no brush, stable operation, small frequency converter capacity, variable frequency factor, etc. [1]. This kind of machine can be used in variable-speed constant frequency system and high capacity variable-frequency speed control system.

Direct torque control (DTC) has features of simple structure, fast dynamic-response torque, good robustness and low-reliability on machine parameters, which solve the problems about complicated structure, large amount of calculation and sensitive to parameter change of vector control [2]. According to the instantaneous error of torque and flux linkage to choose voltage vector, traditional DTC uses a two hysteresis controller and a voltage vector table meter to control torque and flux linkage with simple structure and fast dynamic torque response ability. But the weakness is only one useful voltage vector in each control cycle, that cannot completely compensate the error of torque and flux linkage, then large ripple will occur [3].

To solve the problems of torque ripple in DTC, scholars from all over the world did a lot of research

and put forward many improvement methods, such as using the voltage space vector modulation (SVM-DTC) [4], the discrete space voltage vector [5], fuzzy control [6,7], and predictive control [8]. All these methods can reduce the torque ripple. The SVM-DTC algorithm in ref. [4] can effectively reduce the torque ripple but requires a large amount of calculation and more parameters. The discrete space vector (DSVM) in ref. [5] has the advantage of good robustness in direct vector control, but the improvement of control accuracy is based on the premise of breakdown voltage vector which increased the complexity of the control system. In ref. [6], a fuzzy control algorithm is presented and has a good dynamic performance, which effectively reduces the torque ripple. But in the state machine, variable membership has uncertainty; if membership choice is not appropriate, the system's performance will be worse. In ref. [7], using the improved fuzzy DSVM-DTC control method improved the control of torque and speed, but the fuzzy controller adopts five inputs and the control rules are very complex. The torque prediction is used in ref. [8], which reduces torque ripple and improves the waveform of stator current, but needs complex calculation and the calculation amount is huge.

The DTC method based on duty ratio modulation means that the non-zero voltage vector only acts partial time in one control cycle and zero voltage vector acts on the rest time [9]. This study presents a method of com-

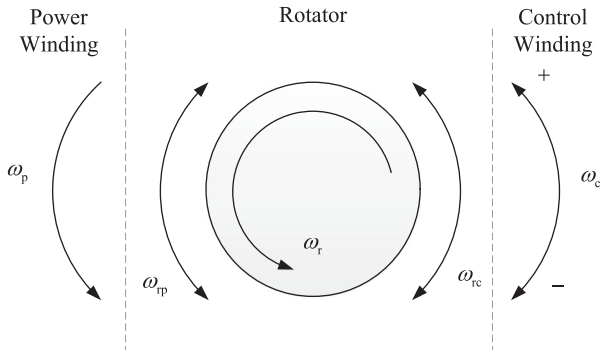


Figure 1. Interaction among internal rotating magnetic fields of BDFM.

binning prediction control and duty ratio modulation to reduce torque ripple, which is based on analysing the ripple causes of traditional DTC, combing the state function of BDFM and model prediction theory of DTC. Using the torque at the current moment, the predicted torque at the next moment, and the selected non-zero voltage vector, the optimal operating time for the non-zero voltage vector and the zero voltage vector in one control cycle is calculated. Through the experiments of proposed control method and compared with traditional DTC, this method can reduce torque and flux linkage ripple.

2. Analysis on torque ripple of BDFM

2.1. Basic electromagnetic relation of BDFM

The inner electromagnetic relation of BDFM is complex because of the two sets of stator winding with different poles. Figure 1 shows interaction of BDFM rotating magnetic fields. Counterclockwise is positive, BDFM is running on the super-synchronous state when the magnetic field of control winding is rotated counterclockwise, other as BDFM is in the state of sub-synchronization [10].

In the state of stable operation, the operation mode is similar to the winding induction machine with $(p_p + p_c)$ poles, the function of power winding and control winding of BDFM is the same as the function of stator and rotator of winding induction machine. Therefore, the electromagnetic torque of BDFM can be expressed by stator flux linkage [11]:

$$\begin{aligned} T_{em} &= \frac{3(p_p + p_c)}{2\sigma L_c} |\lambda_{pc} \times \lambda_c| \\ &= \frac{3(p_p + p_c)}{2\sigma L_c} |\lambda_{pc}| |\lambda_c| \sin \delta. \end{aligned} \quad (1)$$

In which, p_p , p_c are pole pairs of power winding and control winding, respectively; $\sigma = 1 - M_{pc}^2/(L_p L_c)$ is the leakage factor; L_p , L_c , M_{pc} are power winding self-inductance, control winding self and mutual inductance, respectively; λ_c is the control winding flux

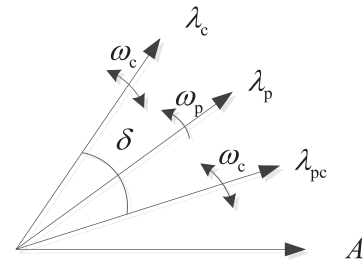


Figure 2. Relationship of flux vectors in stationary reference frame.

linkage vector; λ_p is the power winding flux linkage vector; λ_{pc} is the power winding flux linking the control winding, $\lambda_{pc} = (\lambda_p M_{pc}/L_p)$; δ is the angle of λ_{pc} and λ_c . Figure 2 shows the relation of rotation speed and position of power winding flux linkage λ_p , control winding flux linkage λ_c and the power winding flux linking the control winding λ_{pc} in static coordinate. λ_{pc} is rotating in angel frequency ω_c of control winding current, which is relatively static to control winding flux linkage λ_c [12].

Because the power winding connects to power grid directly, the rotating speed and amplitude of flux linkage λ_p is stable. And $|\lambda_{pc}| = M_{pc} |\lambda_p| / L_p$ can come out the amplitude of λ_{pc} is a constant value.

2.2. DTC of BDFM

In Figure 3, traditional DTC consists of two hysteresis controllers, torque and flux observers and a voltage vector table. DTC scheme establishes mathematical model based on rotator speed $d-q$ coordinate, through measuring the voltage and current of BDFM and the coordinate transformations to calculate magnetic torque, flux amplitude and angle. The measured torque and flux are compared with references and the errors are fed to two hysteresis comparators.

After lookup, voltage vector table based on torque error, flux error and flux section to selected corresponding voltage vector to limit torque error and flux error in hysteresis band, respectively. But there is only one vector that reacts in a controlling period; so it cannot compensate torque error and flux error accurately because the direction of flux error is arbitrary when BDFM is running [9,10].

The influence of selected voltage vectors on electromagnetic torque and flux in sector I can be seen in Figure 4.

2.3. Ripple analysis of DTC

From the formula (1), electromagnetic torque T_{em} is determined by the product of control winding flux linkage amplitude $|\lambda_c|$, the power winding flux linking the control winding linkage amplitude $|\lambda_{pc}|$ and vector angle δ [10]. Linkage amplitude $|\lambda_c|$ and $|\lambda_{pc}|$

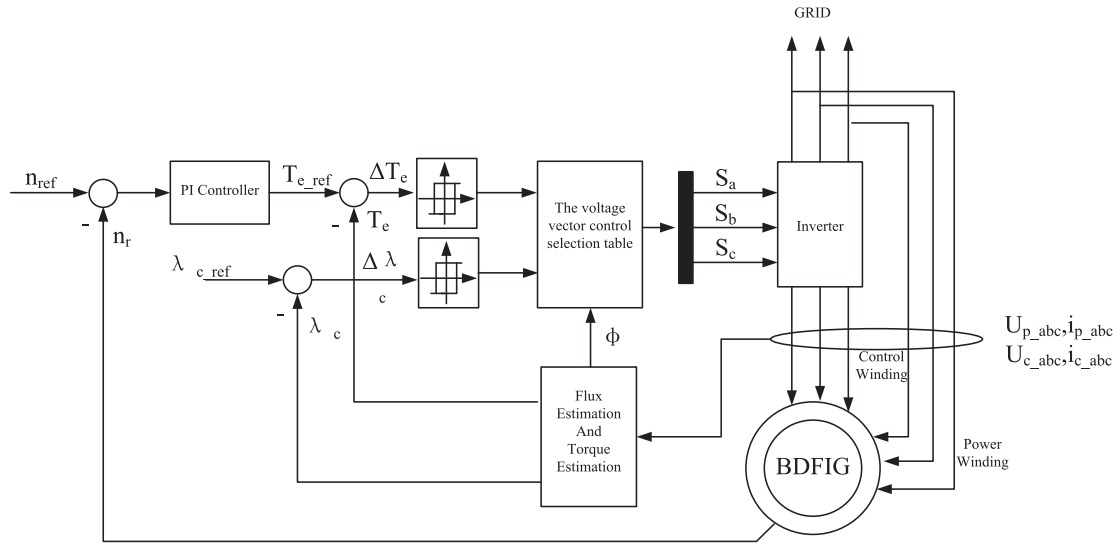


Figure 3. The block diagram of traditional DTC system.

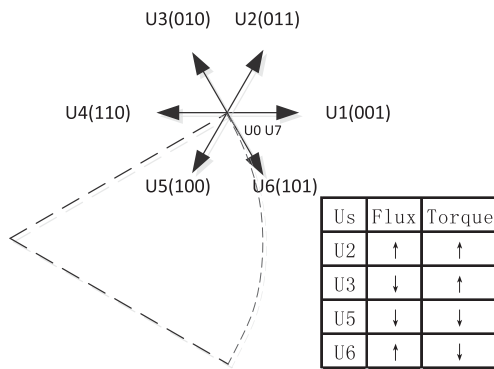


Figure 4. The effect of voltage vectors on flux and torque.

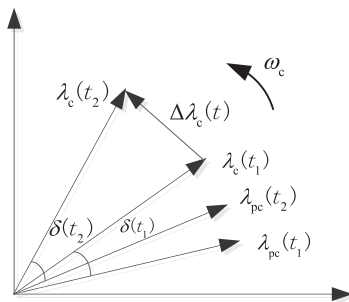


Figure 5. Impact of voltage space vector of control wind on torque.

remain nearly unchanged in the state of stable operation of BDFM. Therefore, the control of electromagnetic torque T_{em} can be realized by using the voltage vector U_c to control the flux rotation speed of control winding and change the vector angle δ in DTC [13].

For the super-synchronous operation of BDFM, Figure 4 indicates the control winding voltage vector effects on electromagnetic torque. The control winding flux linkage $\lambda_c(t_1)$, the power winding flux linking the control winding $\lambda_{pc}(t_1)$ and angle vector $\delta(t_1)$ at t_1 are shown in Figure 5.

From t_1 to t_2 , under the voltage of U_c (110), control winding flux linkage rotates from $\lambda_c(t_1)$ to $\lambda_c(t_2)$, the amplitude $|\lambda_c|$ is nearly stable, and flux linkage follows the voltage vector. In this period, the λ_{pc} rotating speed is restricted by angle frequency ω_c of control winding current. λ_{pc} changes from $\lambda_{pc}(t_1)$ to $\lambda_{pc}(t_2)$, vector angle δ increases from $\delta(t_1)$ to $\delta(t_2)$ rapidly, and electromagnetic torque T_{em} increased [14].

Applied a zero voltage vector at t_2 , control winding flux linkage $\lambda_c(t_2)$ keeps in the same position, and λ_{pc} rotates at the speed of ω_c , then the vector angle δ and T_{em} decreased.

For the traditional DTC, hysteresis comparator cannot distinguish the size of torque and flux linkage error. Controller applies voltage vector to the whole control cycle. In the cycle with smaller torque error, the voltage makes the torque to achieve a given value quickly in a short time, and unchanged switch state of inverter makes torque along the original direction, then huge torque ripple occurred [9].

3. The control scheme of DTC based on duty ratio modulation

Based on the analysis above, the effective method to reduce large torque ripple is to control the effective function time of effective voltage vector [14,15]. Among the control methods proposed in this paper, assume that t_{sp} is the period of one control cycle, non-zero voltage vector function only partial time, other time use zero voltage vector to control, and the actuation time of non-zero and zero voltage are t_s , $t_{sp}-t_s$.

When the rotating torque needs to be increased, we chose a non-zero voltage vector from voltage vector table, this voltage vector makes control winding flux linkage λ_c rotate relatively to λ_{pc} , and the vector angle δ and torque increased. To decrease the torque, we

chose a zero voltage vector, control winding flux linkage λ_c stops rotating, λ_{pc} continues rotating slowly and δ decreased, torque decreased.

3.1. Calculation of non-zero voltage vector actuation time t_s

In one control period, through control the action time of non-zero voltage vector can decrease the torque ripple. Because there is no direct coupling between power winding and control winding of BDFM, mutual induction M_{pc} between power winding and control winding cannot be calculated, then non-zero voltage vector actuation time t_s cannot be found through above analytical methods [16,17].

Through transforming the math model of BDFM rotor speed d - q coordinate, the state equation obtained is as follows [12]:

$$\dot{\mathbf{x}}(t) = \mathbf{A}\mathbf{x}(t) + \mathbf{B}\mathbf{u}(t) \quad (2)$$

in which $\mathbf{x}(t) = [i_{qp}(t) \ i_{dp}(t) \ i_{qc}(t) \ i_{dc}(t) \ i_{qr}(t) \ i_{dr}(t)]^T$ are the dq current components of power winding, control winding and rotator, respectively. $\mathbf{u}(t) = [u_{qp}(t) \ u_{dp}(t) \ u_{qc}(t) \ u_{dc}(t) \ u_{qr}(t) \ u_{dr}(t)]^T$ are the dq current components of power winding, control winding and rotator, respectively. $\mathbf{A} = [\mathbf{A}_1 \ \mathbf{A}_2 \ \mathbf{A}_3 \ \mathbf{A}_4 \ \mathbf{A}_5 \ \mathbf{A}_6]^T = -\mathbf{L}^{-1}\mathbf{R}$, $\mathbf{B} = [\mathbf{B}_1 \ \mathbf{B}_2 \ \mathbf{B}_3 \ \mathbf{B}_4 \ \mathbf{B}_5 \ \mathbf{B}_6]^T = \mathbf{L}^{-1}$,

$\mathbf{A}_i, \mathbf{B}_i (i = 1 \sim 6)$ is a 1×6 matrix,

$$\mathbf{L} = \begin{bmatrix} L_{sp} & 0 & 0 & 0 & M_{pr} & 0 \\ 0 & L_{sp} & 0 & 0 & 0 & M_{pr} \\ 0 & 0 & L_{sc} & 0 & -M_{cr} & 0 \\ 0 & 0 & 0 & L_{sc} & 0 & M_{cr} \\ M_{pr} & 0 & -M_{cr} & 0 & L_{sr} & 0 \\ 0 & M_{pr} & 0 & M_{cr} & 0 & L_{sr} \end{bmatrix},$$

$$\mathbf{R} = \begin{bmatrix} R_p & p_p \omega_r L_{sp} & 0 & 0 \\ -p_p \omega_r L_{sp} & R_p & 0 & 0 \\ 0 & 0 & R_c & p_c \omega_r L_{sc} \\ 0 & 0 & -p_c \omega_r L_{sc} & R_c \\ 0 & 0 & 0 & 0 \\ & & 0 & p_p \omega_r M_{pr} \\ & & -p_p \omega_r M_{pr} & 0 \\ & & 0 & p_c \omega_r M_{cr} \\ & & p_c \omega_r M_{cr} & 0 \\ & & R_r & 0 \\ & & 0 & R_r \end{bmatrix}$$

where R_p, L_p, M_{pr} are the power winding resistance, self-inductance and the mutual inductance with rotator, respectively; R_c, L_c, M_{cr} are the power winding resistance, self-inductance and the mutual inductance with rotator, respectively; R_r, L_r, ω_r are the rotator resistance, self-inductance and mechanical angle speed, respectively.

After the discretization of first-order forward Euler method (2), the following equation can be obtained [16]:

$$\begin{aligned} \mathbf{x}(k+1) &= [\mathbf{I} + \mathbf{A}t_{sp}]\mathbf{x}(k) + \mathbf{B}t_{sp}\mathbf{u}(k) \\ &= \mathbf{I} \cdot \mathbf{u}(k) + [\mathbf{A}\mathbf{u}(k) + \mathbf{B}\mathbf{u}(k)]t_{sp} \end{aligned} \quad (3)$$

in which \mathbf{I} is a six-order unit matrix; t_{sp} is the control cycle.

Through u - i flux observer [8]

$$\lambda = \int (\mathbf{u} - \mathbf{i}R)dt \quad (4)$$

after discretization

$$\lambda(k+1) = \lambda(k) + [\mathbf{u}(k) - \mathbf{i}(k)R]t_{sp}. \quad (5)$$

The flux linkage of power winding and control winding at the moment of $(k+1)$ are:

$$\begin{cases} \lambda_{qp}(k+1) = \lambda_{qp}(k) + [u_{qp}(k) - i_{qp}(k)R_c]t_{sp} \\ \lambda_{dp}(k+1) = \lambda_{dp}(k) + [u_{dp}(k) - i_{dp}(k)R_c]t_{sp} \\ \lambda_{qc}(k+1) = \lambda_{qc}(k) + [u_{qc}(k) - i_{qc}(k)R_c]t_{sp} \\ \lambda_{dc}(k+1) = \lambda_{dc}(k) + [u_{dc}(k) - i_{dc}(k)R_c]t_{sp} \end{cases}. \quad (6)$$

Through BDFM electromagnetic torque equation [8]

$$T_{em} = p_p(i_{qp}\lambda_{dp} - i_{dp}\lambda_{qp}) + p_c(i_{qc}\lambda_{dc} + i_{dc}\lambda_{qc}). \quad (7)$$

Put formula (3) and (6) into (7) and discretized, ignore t_{sp}^2 [9], the torque increment $+\Delta T_{em}$ at the moment of $(k+1)$ is shown in the next equations when non-zero voltage vector actuated in the whole control cycle t_{sp} .

$$\begin{aligned} \frac{+\Delta T_{em}}{t_{sp}} &= p_p[i_{qp}(k)(u_{dp}(k) - i_{qp}(k)R_p) \\ &\quad + \psi_{dp}(k)(\mathbf{A}_1\mathbf{x}(k) + \mathbf{B}_1\mathbf{u}(k)) \\ &\quad - i_{dp}(k)(u_{dp}(k) - i_{dp}(k)R_p) \\ &\quad + \psi_{qp}(k)(\mathbf{A}_2\mathbf{x}(k) + \mathbf{B}_2\mathbf{u}(k))]t_{sp} \\ &\quad + p_c[i_{qc}(k)(u_{dc}(k) - i_{qc}(k)R_c) \\ &\quad + \psi_{dc}(k)(\mathbf{A}_3\mathbf{x}(k) + \mathbf{B}_3\mathbf{u}(k)) \\ &\quad - i_{dc}(k)(u_{dc}(k) - i_{dc}(k)R_c) \\ &\quad + \psi_{qc}(k)(\mathbf{A}_4\mathbf{x}(k) + \mathbf{B}_4\mathbf{u}(k))]t_{sp} = f_1. \end{aligned} \quad (8)$$

where, f_1 is the torque variation slope with non-zero voltage vector.

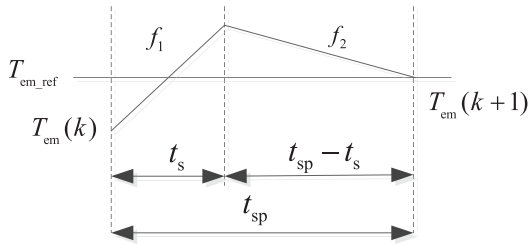


Figure 6. Diagram of ratio determination methods.

The torque increment $-\Delta T_{em}$ at the moment of $(k+1)$ is shown in the next equations when zero voltage vector actuated in the whole control period t_{sp} .

$$\begin{aligned} \frac{-\Delta T_{em}}{t_{sp}} = & p_p [i_{qp}(k)(u_{dp}(k) - i_{qp}(k)R_p) \\ & + \psi_{dp}(k)(A_1 \mathbf{x}(k) + B_1 \mathbf{u}(k)) \\ & - i_{dp}(k)(u_{dp}(k) - i_{dp}(k)R_p) \\ & - \psi_{qp}(k)(A_2 \mathbf{x}(k) + B_2 \mathbf{u}(k))] t_{sp} \\ & + p_c [i_{qc}(k)(-i_{qc}(k)R_c) \\ & + \psi_{dc}(k)(A_3 \mathbf{x}(k) + B_3 \mathbf{u}(k)) \\ & - i_{dc}(k)(-i_{dc}(k)R_c) \\ & - \psi_{qc}(k)(A_4 \mathbf{x}(k) + B_4 \mathbf{u}(k))] t_{sp} = f_2. \quad (9) \end{aligned}$$

where, f_2 is the torque variation slope with non-zero voltage vector.

Because of the control cycle, t_{sp} is short, the change of flux and speed is small, so the torque change slope f_1 , f_2 can be treated as stable when non-zero and zero voltage vector actuated in one control period. The torque increase and decrease is approximately linear, as shown in Figure 6.

At the end of control period, prospected instant torque is equal to the command torque [17],

$$T_{em}(k+1) = T_{em_ref} \quad (10)$$

in which, $T_{em}(k+1)$ is the instant electromagnetic torque; T_{em_ref} is torque command.

The torque variation in one control period [17] can be expressed as

$$f_1 \cdot t_s + f_2(t_{sp} - t_s) = T_{em_ref} - T_{em,0} \quad (11)$$

where $T_{em,0}$ is the torque initial value at the beginning of control period.

Non-zero voltage vector actuation time t_s can be calculated from formula (11):

$$t_s = \frac{T_{em_ref} - T_{em,0} - f_2 t_{sp}}{f_1 - f_2}. \quad (12)$$

3.2. DTC method based on torque duty ratio modulation

BDFM torque ripple minimize control system is shown in Figure 7, the control strategy is [17]:

- (1) Based on the traditional DTC theory to choose voltage vector;
- (2) Calculate torque change slope f_1 , f_2 in non-zero and zero voltage vector actuation period, respectively, by using formula (8) and (9);
- (3) Calculate non-zero voltage vector actuation time t_s by using formula (12);
- (4) Estimate the value of t_s . When $t_s > t_{sp}$, applied non-zero voltage vector in the whole control period; when $t_s < 0$, applied non-zero voltage in the whole control period; When $0 < t_s < t_{sp}$, applied non-zero voltage in the period $0 \sim t_s$, and applied zero voltage in the period $t_s \sim t_{sp}$.
- (5) At the beginning of next control period, set t to zero, and then repeat the above steps.

4. Experimental results

To validate the proposed torque ripple minimizing control strategy, experimental platform of BDFM was built, as shown in Figure 8. This system uses DC generator as load, uses four CS100A - B3V3 hall sensors to measure the current of power winding and control winding, uses JN338AE rotary incremental encoder to measure machine speed, and resolution is 1024 pulses/roll. Inverter circuit in this system is the PM150RLA120 intelligent power module IPM (from Japanese Mitsubishi electric company). Digital signal processor is the core of control system and communicates with host computer through the serial communication interface RS232 to realize data transmission between DSP and host computer. Host computer use Labview to receive the data of current, rotational speed and torque from DSP, and then stores these data. Inverter switch frequency is 5kHz, the set amplitude of control winding flux linkage is $|\Psi_{c_ref}| = 0.85$ Wb and the moment of inertia is $J = 0.8$ kg m². The short-circuit start is applied at the beginning of experiment, the rotational speed was set into $n_r = 624$ r/min after stable operation, and the speed was set into 636 r/min when machine operated stably with load. The parameters of BDFM are shown in Table 1.

A comparative study on traditional DTC and duty ratio modulation DTC was conducted by using the above experimental platform. During the experiment, BDFM start without load; when the operation became stable, the torque increased to 40 N·m and continued to operate.

Figure 9 shows the rotator speed curve under the duty ratio modulation DTC of BDFM. Control winding was shortened at the start, rotator speed increase to synchronous speed rapidly, the speed was set into $n_r = 624$ r/min at $t = 4.5$ s, and set into 636 r/min at $t = 16.5$ s. The curve in Figure 9 indicates that rotator speed can follow the set speed rapidly.

Figures 10 and 11 show the current differences and torque differences of traditional torque control and the

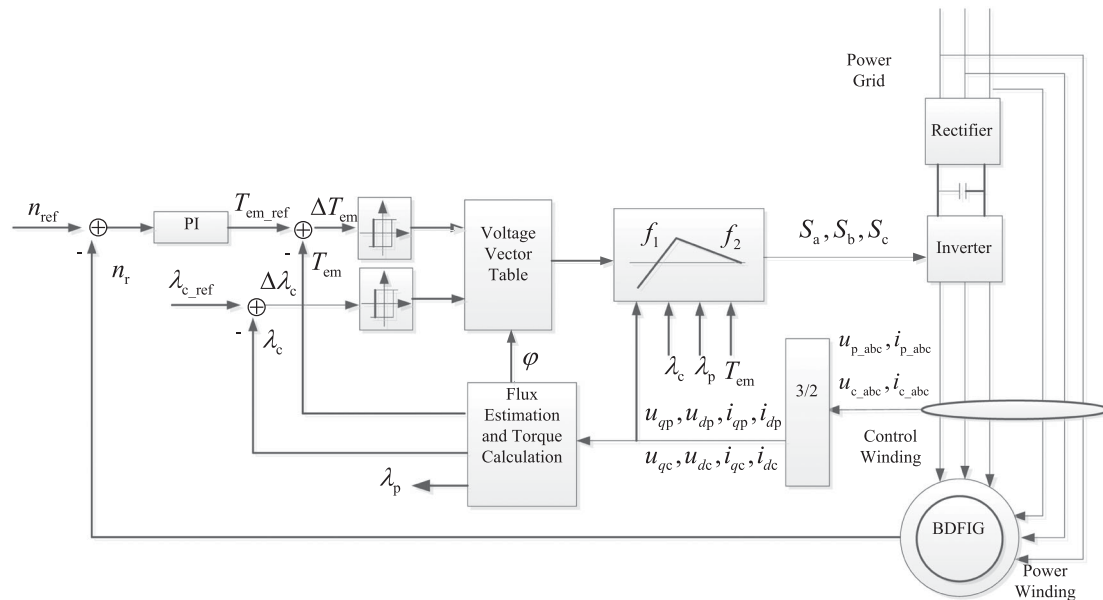
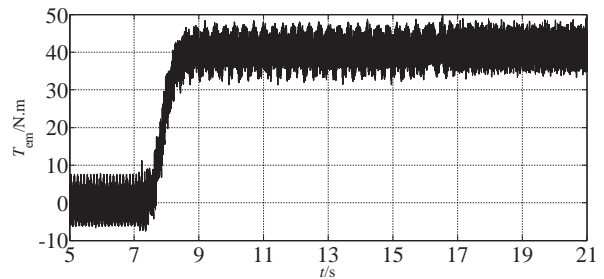


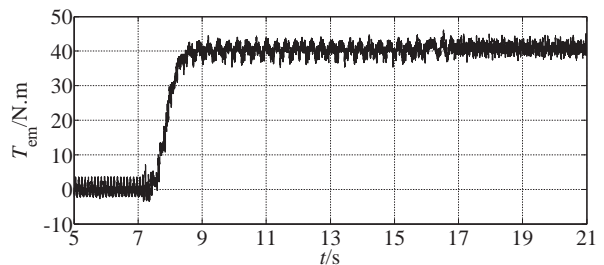
Figure 7. The control block diagram of the proposed duty ratio modulation DTC of BDFM.

Table 1. The parameters of BDFM.

	Power winding	Control winding	Rotor
Self-inductance (mH)	60.4	130.7	18.4
Mutual inductance (mH)	26.8	27.9	
Resistor (Ω)	0.401	0.5009	7.5353×10^{-5}
Pairs	4	1	



(a) Torque in traditional direct torque control



(b) Torque in the control with duty ratio modulation

Figure 10. The torque waveform in steady state. (a) Torque in traditional direct torque control. (b) Torque in the control with duty ratio modulation.

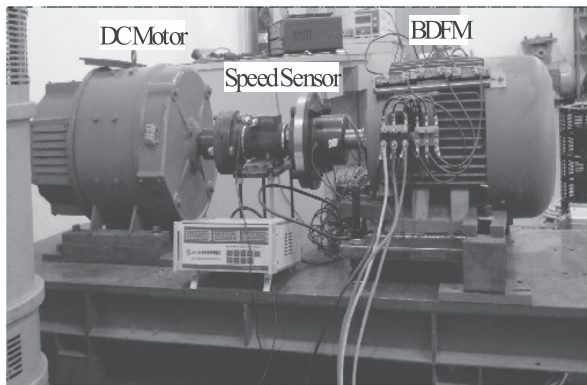


Figure 8. The experimental platform of BDFM.

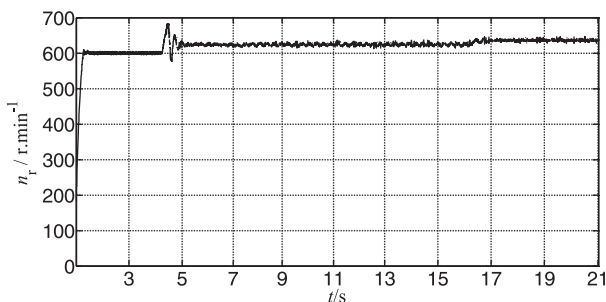


Figure 9. Rotator speed of BDFM.

duty ratio modulation torque control. The load torque increases from 0 to 40 N m at 7 s.

From Figure 10, under the traditional DTC, the selected voltage vector makes torque increase to the set value in the cycles with small torque deviation. This occurs because controller makes selected voltage actuate in the whole period. There is no state change of inverter switch; so torque varies along the original direction, then big torque ripple occurs, which is about 8 N m. Under the DTC with duty ratio modulation, in one control period, the selected non-zero voltage actuation time can be calculated by torque error and

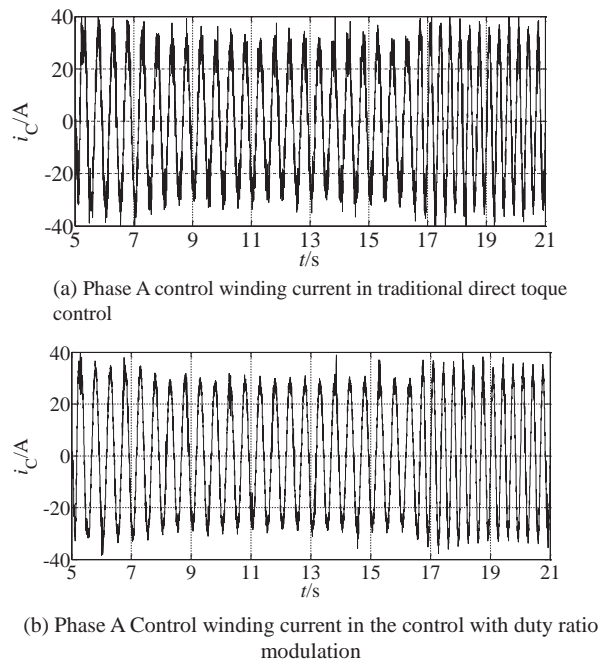


Figure 11. Control winding current of phase A in steady state. (a) Phase A control winding current in traditional direct torque control. (b) Phase A control winding current in the control with duty ratio modulation.

torque change slope, and zero voltage actuates in other time. The torque is about 4 N m, which decreases the torque ripple effectively and then verifies the control method based on duty ratio modulation is effective and feasible.

Figure 11 shows the waveform of BDFM control winding current in steady state, rotor speed is 624 r/min from 5 to 16.5 s, and the current frequency is 2 Hz. In the period 16.5–21 s, the rotor speed is 636 r/min and the current frequency is 3 Hz. For the traditional DTC, control winding current ripple is big because of no switch state change of inverter in the whole control period. But the torque ripple minimization control based on duty ratio modulation can make control winding current smooth and torque ripple small, which is because non-zero and zero voltages actuate, respectively, and non-zero voltage only actuates in the part time of the whole control cycle.

5. Conclusions

For the BDFM, traditional DTC has many problems such as big output torque ripple and uncertain inverter switch frequency. Based on the analysis of traditional DTC, this paper proposed a new torque control which applied duty ratio modulation into DTC. According to the BDFM state equation and the prediction of torque, flux linkage in the next moment and the minimum torque ripple in one control cycle, non-zero voltage actuation time can be found. The results show that the control method can reduce the torque ripple and can keep the advantages of torque fast response and simple

control of traditional DTC as well as improve control performance compared with traditional DTC.

Disclosure statement

No potential conflict of interest was reported by the authors.

Funding

The authors wish to extend their gratitude to State Administration of Foreign Experts Affairs for supporting the project “Overseas Expertise Introduction Program for Disciplines Innovation in Universities” (Ref: B13009), NSFC projects (61571189) and to the Fundamental Research Funds for the Central Universities (2017MS186) project.

References

- [1] Protsenko K, Xu D. Modeling and control of brushless doubly-fed induction generators in wind energy applications. *IEEE Trans Power Electron.* 2008;23(3):1191–1197.
- [2] Habetler WBRS. Direct torque control for brushless doubly-fed machines. *IEEE Trans Ind Appl.* 1996;32(5):1098–1104.
- [3] Domenico Casadei FGAA. FOC and DTC: two viable schemes for induction motors torque control. *IEEE Trans Power Electron.* 2002;17(5):779–787.
- [4] Yanjun G, Nan W. Direct torque control for brushless doubly-fed machine based on SVPWM. *Small Spec Electr Mach.* 2011;39(8):58–60.
- [5] Casadei GSAAD. Improvement of direct torque control performance by using a discrete SVM technique. In: PESC 98 Record. 29th Annual IEEE Power Electronics Specialists Conference; Fukuoka, Japan. 1998. p. 997–1003.
- [6] Fattahi SJ, Khayyat AA. Direct torque control of brushless doubly-fed induction machines using fuzzy logic. *PEDS*; Dec 5–8; Singapore. 2011. p. 619–624.
- [7] Xingjia Y, Lei S, Qingding G. Brushless doubly-fed machine direct torque control based on fuzzy strategy. *J Power Supply.* 2011;11(6):54–58.
- [8] Ai-ling Z, Yang Z. Direct torque control for brushless doubly-fed machine based on torque predict control strategy. *Electr Mach Control.* 2007;11(4):326–330.
- [9] Seung-Ki KJAS. New direct torque control of induction motor for minimum torque ripple and constant switching frequency. *IEEE Trans Ind Appl.* 1999;35(5):1076–1082.
- [10] Shi J. Study on direct torque control technology for variable speed constant frequency brushless doubly-fed wind power generator [PhD thesis]. Shenyang: Shenyang University of Technology; 2011. p. 18–19.
- [11] Jovanović MG, Yu J, Levi E. Encoderless direct torque controller for limited speed range applications of brushless doubly fed reluctance motors. *IEEE Trans Ind Appl.* 2006;42(3):712–722.
- [12] Sarasola I, Poza J, Rodriguez MA, et al. Predictive direct torque control for brushless doubly Fed machine with reduced torque ripple at constant switching frequency. *ISIE.* 2007:1074–1079.
- [13] Joon Hyung Ryu KWLJ. A unified flux and torque control method for DTC-based induction-motor drives. *IEEE Trans Power Electron.* 2006;21(1):234–242.
- [14] Attous DB. Power control of brushless doubly-fed machine based on back-to-back pwm converter in wind

- energy conversion system. *Mediterr J Meas Control*. [2012](#);8(1):351–358.
- [15] Chaal H, Jovanovic M. Power control of brushless doubly-fed reluctance drive and generator systems. *Renewable Energy*. [2012](#);37(1):419–425.
- [16] Feng N, Kui L, Yao W. Model predictive direct torque control for permanent magnet synchronous machines based on duty ratio modulation. *Trans China Electrotech Soc*. [2014](#);29(11):20–29.
- [17] Feng N, Kui L, Yao W. Direct torque control for permanent-magnet synchronous machines based on duty ratio modulation. *IEEE Trans Ind Electron*. [2015](#);62(10):6160–6170.